ISSN 2455-4863 (Online) **www.ijisset.org** *Volume: 4 Issue: 12 | 2018*

Ultramafic rock of carbonatite complex of Tiruppattur India

R. Ramasamy

Retired Deputy Director, Tamil Nadu State Department of Geology and Mining, Chennai, 600032, India

Abstract: *- Ultramafic rock (**um**) occurring in carbonatite complex of Tiruppattur (12° 00'00"-12°30'00"N and 78°25'00"-78°35'00"E) includes dunite, peridotite, and pyroxenite. Normative composition of **um** appears to be derived by alteration of peridotite. It is enriched with MgO and Al_2O_3 components but poor in CaO. Part of CaO is released out as carbonates from **um.** Normative clinopyroxene exceeds over olivine. Conversion of olivine into clinopyroxene- amphibole-biotite and spinel increases normative quartz content. Absence of accessory plagioclase indicates that **um** might have been formed at higher PTX above stability field of plagioclase in mantle. Plagioclase component at mantle PTX condition in **um,** anorthite / albite break down into tschermakite and quartz. Formation of tschermakite may be caused enrichment of SiO_2, Al_2O_3, Na and Fe''' in residual **um.** Under subsolidus silica undersaturated residual **um** transforms continuously tschermakite –gehlinite- meionite and calcite. On the other hand albite may be replaced into jadeite, acmite-calcite- soda melilite and meionite. The reversible process of transformation at low PTX of tschermakite by absorbing quartz transforms into anorthite / albite-jadeite into nepheline + albite, tschermakite, melilite, meionite acmite and albite at low PTX conditions at crust. These processes lead to silica undersaturation or oversaturation in **um**. Silica undersaturation in **um** is compensated by entry of non-silicate minerals and alumina bearing minerals at high PTX at mantle. Volatiles in mantle can be present as inclusions or bubbles in subsolidus mantle reduce rigidity of substratum column. The Increasing volume of volatiles reduces formation of nepheline and other silica undersaturated minerals. Mineralization of vermiculite, apatite, monazite, zircon, hercynite, nioborutile, REE bearing minerals exhibits evidence for alumina enrichment in **um**. The composition ranges of end members pyroxene (wollastonite-enstatite- ferrosilite) – jadeite - aegirine lead to subsolidus differentiate into two different trends of mafic and feldsic / alkaline rock evolution from mantle source to crust under their inherent PTX.*

Keywords: Carbonatite complex of Tirupattur, Alumina rich Ultramafic, Tschermakite-Jadeite-Acmite, Subsolidus mantle differentiation

1. INTRODUCTION

Ultramafic rock ***(um)*** encloses alkali syenites at three different sites in carbonatite complex of Tiruppattur (12° 00' 00"-12°30'00"N and 78°25'00"-78°35'00"E) Tamil Nadu India. Many detailed studies are made on the carbonatite complex of Tiruppattur [1-9] but none of study is published on ***um*** occurring in this complex. The present paper focus on ***um*** to trace mode of occurrences of Mg-Al-Si rich ***um*** and their phase modifications under different PTX conditions.

2. METHODOLOGY

Field works were carried out several times for Ph.D. research-work under the guidance of Dr. S. Saravanan, Head of the Department of Geology, Presidency College, Chennai, between July 1967 and July 1973 on this carbonatite complex [1-4]. After joining the Tamil Nadu State Geology Branch, Department of Industries, exploration and prospecting for vermiculite, sulphides, iron oxides and ultra-pottassic rocks were carried out by the author in this area between January 1974 and June 2000 on various occasions. Floats of iron oxide samples were collected on ***um*** to estimate Al''', incompatible-elements and REE contents. Thin sections of co-magmatic alkali syenites were studied. The enrichment of alumina and magnesia in ***um*** were determined by standard wet-gravimetric analyzes and EDAX spot analyses of samples of ***um*** in the Metallurgical and Material Science Laboratory, IITM by using high resolution scanning electron microscope. Pieces of ***um*** show Mg-Al-Si mineral constituent at various sites estimated. The chemical composition of ***um*** varies one site to another in the same sample. Alkali rich pyroxene (soda-augite, aegirine-augite and acmite) and amphibole (riebeckite, richterite, arfvedsonite and kataphorite) are also found in some other ***um*** in different places in this complex. Alkali component is enriched at contact of carbonatite with ***um*** or alkali syenites. Major and trace elements in ***um*** were determined and interpreted. Rittmann's norms [10] were calculated for major elements.

3. FIELD AND PETROGRAPHIC STUDIES

Ultramafic rock (***um)*** occurring in this area includes dunite, peridotite, harzburgite, leherzolite, websterite, pyroxenite, shonkinite and lamprophyre. Dunite grades into peridotite which further grades

imperceptibly into harzburgite, leherzolite, websterite and pyroxenite. The ***um*** occurs as an arc shaped body, on flanks of carbonatite and alkali syenites near Sevvattur village, alkaline components are enriched [4]. Vermiculite and apatite are mineralized. Very coarse-grained grained soda-pyroxene >10 cm^3 is seen. Vermiculite booklets ±10x8x3cm are seen for a depth over 20m. Apatite is mineralized along with vermiculite. Hydrothermal alteration of thin green coloured phlogopite plates associated with vermiculite might have been caused for this vermiculite deposit. A large body of ***um*** exposing over 24 km^2 is seen in the southwestern part of the carbonatite complex (Fig.1). It encloses riebeckite-syenite and other co-magmatic variants of zircon or garnet bearing alkali syenites.

Fig. 1: Simplified map showing arc-like outcrop of ***um*** in the SW portion of the alkaline complex of Tiruppattur (Ramasamy, 1973 [2], 1982 [3], 2012 [4])

The ***um*** body is an over-turned (Fig.1) doubly plunging basin. Thin veinlets of brown coloured ankerite-carbonatite are exposed south of Olaipatti village. Again barium bearing carbonatite, beforsite, benstonite-carbonatite, and sovite veinlets are also found in this place within ***um***. A very small body of barite 200x 15 cm is exposed for 100 m south of Onnakarai village. Apatite-magnetite rock exposes as small diatreme 1 km NE of Mottusulakkarai in ***um***. The ***um*** occurs as coarse-grained, medium-grained, and fine-grained rocks. It also exhibits porphyritic and vesicular textures [7]. During examinations of thin sections under polarizing microscope no accessory minerals of plagioclase or alkali feldspars are seen in ***um*** except shonkinite which is composed of 50% sanidine and 50% of mafic minerals (Fig.2) mainly augite and olivine. Chrysotile veinlets are found along a shear zone trending NE-SW direction about 500m west of Mottusulakkarai village where beforsite carbonatite is exposed.

EDAX images show overlapping large plates of pyroxene grains (50x50x1 µm) one over other. The interval between these plates varies between 1 and 5 µm. Some pyroxene clots have very fine fibrous chrysotites (Fig.3) 0.05 x 5 µm are developed.

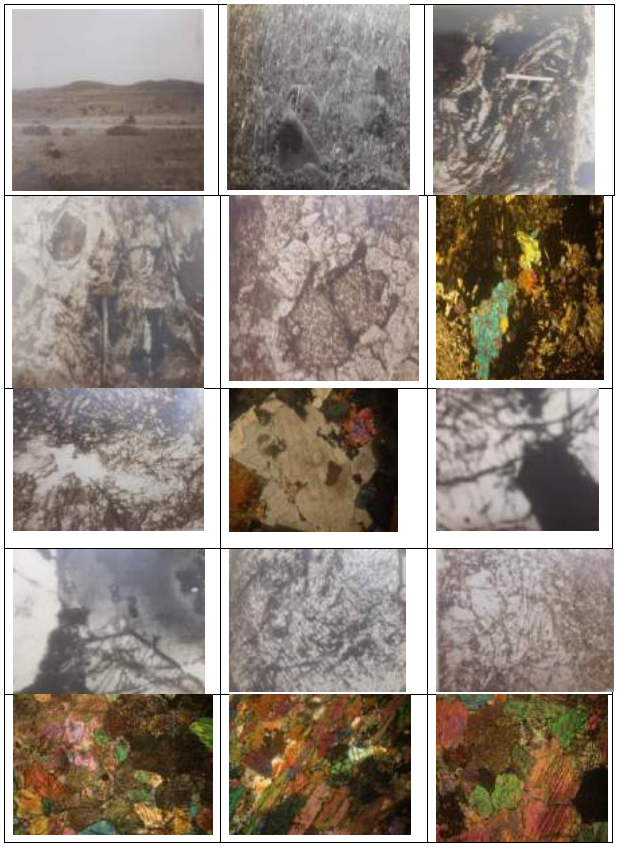

Fig. 2: Field exposures and thin sections of under polarizing microscope (left to right) 1: about 30 m high dunite- peridotite hillocks capped by magnesite and laterite 2: shonkinite exposure in 1967 3: folded pattern of skarn rock 4: ultrabasic nodule in skarn 5: replacement of diopside into andradite calcite at its peripheral portion 6: garnet bearing ***um*** nodule in skarn, 7: reaction texture in skarn 8: sanidine and aegirine augite bearing shonkinite 9: pseudomorph of magnetite after olivine 10: olivine and iron oxide clouded in sanidine (shonkinite) 11: release of iron oxide from diopside in pyroxenite 12: altered pyroxene in pyroxenite 13: development of amphibole in pyroxenite 14: flakes of phlogopite is seen in phlogopite-pyroxenite 15: clinopyroxene carrying amphibole, magnetite and garnet.

ISSN 2455-4863 (Online) **www.ijisset.org** *Volume: 4 Issue: 12 | 2018*

An arc-shaped skarn rock is exposed along contact between [7] garnet-syenite and ***um***. It exhibits highly folded and deformed structure. It carries ultrabasic nodules of varying between 0.5 and 50 cm.

Fig.3: EDAX images show grain size, texture and mutual relationship of pyroxene grains in ***µm***. The images show steeply dipping cross-cutting pyroxene crystals; rectangular shaped intergranular cavities with steep walls; enveloping growth of pyroxene; steep and shallow dipping growth of pyroxene grains are also found in some other sample.

The fold pattern of nodule and skarn is very similar (Fig. 2) to each other. Thickness of lamina varies between >1 and 10 mm with folded structure is visible even in naked eye. The folding pattern of nodule is produced by making it as independent nodular form comprising with alternative tight dome and swelling basin in a single nodule. The nodule is comprised partially or completely replaced by calcite, wollastonite, melilite and scapolite in swelled basins and granular garnet meionite and diopside in narrow and tightly folded adjacent dome. Native copper, silver, galena, pyrite, phyrrhotite, chalcopyrite, bornite are seen along axial planes of the laminas located mostly along domal anticline-axes. The intensity of transformation is increased from SW to NE. Arc-shaped skarn rock trends from N 20-S200^{o} to N60-240^{o} dipping steeply inward from NW to SE It has more than 200m width in the north-east and less than 5 m width southwest near Onnakarai village and the length exceeds over 2 km. Ankerite carbonatite veinlets <500 x 10 cm and breccias of <100 x 5 cm are [7] seen along some fractures in the skarn. Albitite exposed adjacent to skarn carries galena, monazite and other REE minerals. Skarn at Kodamandapatti village is located 8 km NW of the skarn is independent body but contains no such ***um*** nodules except some green patches. Several parallel pottassic or albitite myrolytic syenites of 2 to 5 m width extending over 200 m length are emplaced along parallel shear zones present in the NW part of the ***um*** arc.

Series of co-magmatic older soda rich and younger potash rich alkali syenites are emplaced in two adjacent structural basins in a sequential order in north and south with magmatic continuity [3]. Soda rich alkali syenites are imperceptly grade into younger porphyritic syenites towards center of the northern basins where porphyritic hornblende syenites further grades into coarse-grained augite-porphyritic syenites in the southern portion of this basin. South of Jogippatti village a ring dyke of carbonatite partially enclosed by ***um*** composed more than 60% of richterite is seen. The southern basin is composed of series of riebeckite-anorthoclase pegmatite and aplite showing myrolytic texture. Agpaitic texture is seen in syenite [4] with development of riebeckite at peripheral portions of feldspars. Aplitic syenites exposed adjacent to Jogipatti ring complex of carbonatites carries meionite scapolite. Pottassic and soda aplites are seen in ***um*** rocks trending E-W direction. Aplites exhibit poikilitic texture with zoned phenocryst of oligoclase (0.4x0.3 mm) to albite. Irregular oscillatory compositional zoning is exhibited among co-magmatic alkali syenites emplaced in this southern basin. Further south anorthoclase-garnet-syenite is exposed. Layers of wollastonite-sovite, wollastonite bearing pegmatite, scapolite-garnet-calcite bearing aplite and wollastonite monomineralic rock are found. Very fine-grained silica undersaturated microcline-melanite syenite and

lamprophyric shonkinite at peripheral portion of ***um*** are seen [2, 3, 4]. Small veins of anorthoclasite, albitite, syenite porphyries and apatite-magnetite rocks occur as thin veins in ***um***. Zircon syenite occurs as a small plug 2 km SW of Samalpatti village. Semi-precious zircon crystal occurs as accessory mineral in the carbonatite of Sevvattur.

Pyroxenite is hard and compact rock. It is amphibolized and biotitized at several places [7]. The shonkinite dyke exhibits panidiomorphic texture. It is a coarse-grained rock and is composed with euhedral minerals. Two generation of olivine, augite, amphibole phlogopite, magnetite and sanidine occur as phenocrysts and matrix. Some brown coloured lamprophyre is composed of euhedral clinopyroxene (0.8-0.5mm) amphibole (0.4x1.2 mm) amidst fine-grained clayey matrix derived by alteration of phlogopite. The latter occurs as diatremes along ***um*** near Garigaipalli village along railway-line cuttings.

Massive part of dunite and peridotite shows equigranular and sacchoroidal texture and the size of mineral grains around 1mm. Magnesite or lime material is released out along rhombohedral cleavages developed by deformation. At some places along these cleavages large porphyric pyroxene / amphibole is seen. Porphyritic pyroxenite is composed of large grains of pyroxene or amphibole over 5 cm in fine-grained pyroxenes matrix are seen. Phlogopite of 0.1 to 5mm occurs as accessory mineral along cleavage and joint plane of pyroxenite. Secondary calcitic encrustations are found along these cleavages. The EDAX image shows large pyroxene grain of size varying between 0.1 and 10 mm sequentially altered to amphibole, biotite, and vermiculite to iron oxides are seen. The iron oxide ultimately washed out leaving empty spaces [7] and cavernous structure is developed in ***um***. Some cavities are interconnected and some others are not interconnected but filled with vermiculite or iron oxides. The development of such alteration in very coarse-grained ***um*** is also seen but rare. It exhibits inequigranular texture. It is largely composed of olivine, diopside, hornblende and biotite. The sizes of mineral grains and their mutual relationship may be estimated by using their photomicrographs and EDAX images. Initial development of rhombohedral cleavage is often filled with carbonate material leached out. The released Mg rich and Ca poor carbonate materials are deposited along cleavage planes. Ca is mostly utilized for formation of secondary carbonate, anhydride, apatite and halides. Fe ions are utilized for Sc, Cr and Y oxides and Fe, Co, Ni, Cu ions for their mineralization in combination with carbonate and sulphide. The magnesia content increases due enrichment of forsterite content in olivine or enstatite content and crystallization of magnetite using ferrous iron in pyroxene in saturated norm. Al‴ enters in tschermakite molecules in pyroxene and amphibole. It concentrates in biotite and vermiculite with release of lime and quartz. The syenites exhibit hypidiomorphic granular texture. Vogesite and shonkinite show panidiomorphic texture with euhedral grains of one or more generations of mafic and feldsic minerals.

Wet gravimetric analyses show enrichment of alkalis and volatiles (Table 1). Spot EDAX analyses minerals present ***um*** are shown in Table 2 and their images are presented in Fig.4. Minerals have plate like intergrowths with intergranular linear rectangular cavities varying between 2 and 10 μm. They are steeply dipping inside overlapping one platelet (8x 1 μm) over another and their thickness are often between < 0.5μm and 5μm. Some platelets are interpenetrating. The platelets orient towards various directions for length of 10μm. Their growth and reaction pattern are seen in some pyroxene grains appears to be magmatic. Minimum size of pyroxene crystal is 2 x 0.5 μm. Notable amount of vacant spaces are present between intergranular boundaries of mineral grains. The shape of these spaces vary square, rectangular and narrow lenticular with depth ranging between 0.5 and 2 μm.

4. GEOCHEMICAL STUDIES

Wet-gravimetric chemical analyses are made for fine-grained dunite, pyroxenite and apatite-magnetite bearing pyroxenite (Table 1; Fig. 4.). The degree of oxidation ratio (Fe‴/ (Fe‴ +Fe″+Mn) ranges between 0.19 and 0.93 and the mean value is 0.47. Notable amount of normative ilmenite is present. The low degree of oxidation and enrichment of alkalis, formation of magnetite is limited. Considerable amount of potash is present over soda. Mean proportions of olivine and pyroxene is 29.22 and it indicates that -

peridotite being the source rock for pyroxenite. MgO content exceeds over FeO. Normative olivine and feldspar rich pyroxenite yields nepheline. The ***um,*** enriched with amphibole, biotite, spinel and calcite is silica oversaturated.

EDAX analyses Al_2O_3 ranges between 31.58% and 53.65%. Mg exceeds over 11 times of Fe. The presence of CO_2 F, Cl, SO_3 and P_2O_5 produce carbonate, fluoride, chloride, phosphate and anhydride using Ca, Mg, Na, K and P ions. K ions exceed over Na ions. Rb ions are present as trace constituents. F ions exceed over Cl ions. Plots of Sr against Rb or Cr against Sc show perfect positive linear correlation. Fe+Co+Ni+Cu ions against (Fe’”+Sc+Cr+Y) show similar pattern. Fe’”and Al’” ions have negative linear correlation. The incompatible elements such as Sc, Ti, V, Cr, Y, Zr, Nb, Mo, La, Hf and Ta are closely related with each others in their electronic configuration and chemical properties. They are usually concentrated at late magmatic stages. Such elements are mobile under high temperature viscous state of ***um*** at mantle. Significant amount of volatiles such as H_2O, CO_2, CH_4, F, Cl, SO_3, and P_2O_5, and liquid CO_2, are present at higher oxidation fugacity.

Table- 1: Wet-gravimetric analyses various types of pyroxenite

	biopx203	biorieb320	biofelspx32	anpx319	mipx318	pxnod497	olpx40	perido31	bifelpx9	pxcc7	riebcc401	riencc402	biopx736	ccpx29	pxmt460	pxsev11	pxsam500	pxsam501	pxsam502	pxsam503
SiO2	45.82	44.12	21.02	41.26	52.92	45.92	42.38	30.09	36.88	40.85	42.36	46.4	52.4	37.71	13.84	46.77	54.65	38.09	45.21	46.41
Al2O3	15.53	9.1	1.64	3.65	12.98	6.12	4.62	2	1.47	0.74	1.27	10.41	12.26	0.12	0.91	2.17	1.01	5.17	1.28	2.09
Fe2O3	1.5	3.64	5.48	10.18	5.31	5.52	6.32	19.09	15.49	10.33	7.54	9.31	2.99	8.46	28.94	3.43	0.85	1.05	0.9	1.64
FeO	5.59	1.26	2.87	8.26	1.8	5.53	5.25	6.95	10.72	0.57	1.98	2.87	6.75	3.29	17.6	12.58	4.12	14.1	4.32	2.9
Mno	0.19	0.06	0.63	0.29	0.11	0.18	0.15	0.79	0.1	0.13	0.19	0.22	0.02	0.15	0.19	0.13	0.15	0.18	0.09	0.1
MgO	3.95	14.2	6.39	9.67	3.21	9.6	10.62	9.91	8	19.08	12.97	8.32	6.01	8.71	5.42	14.02	17.17	14.18	14.82	14.46
CaO	9.62	21.78	31.68	20.18	6.18	22.46	25.08	15.68	17.76	7	15.65	12.42	8.48	21.1	15.42	19.76	21.37	15.52	20	18.9
Na2O	5.27	1.16	1.96	0.41	2.03	1.08	0.34	3.67	1.53	0.4	4.59	3.04	3.11	0.32	0.06	0.19	0.44	0.23	2.34	2.55
K2O	5.16	1.24	1.44	1.2	11.76	0.18	0.06	0.01	1.88	0.01	0.9	4.38	4.26	2.93	0.14	0.35	0.12	3.44	0.28	0.74
TiO2	0.66	0.88	0.45	1.4	1.09	1.26	0.93	0.63	1.74	0.01	0.44	0.04	0.99	0.75	0.01	0.66	0.22	1.66	0.23	0.17
P2O5	0.33	0.1	0.01	0.73	0.46	0.19	3.1	1.29	1.97	0.01	0.1	0.44	1.53	0.09	0.01	0.33		3.69	0.05	0.74
CO2	4.66	1.12	23.65	0.41	2.24	1.02	0.6	8.93	1.1	20.65	9.75	0.17	0.49	16.6	0.01		0.02		9.68	0.73

	1	2	3	*4*	*5*	*6*	*7*	8.00	*9*	*10*	*11*	*12*	*13*	*14*	*15*	*16*	*17*	*18*	*19*
cc	11.55	2.75	57.40	1.07	5.69	2.63	1.61	19.33	2.36	49.01	24	0.45	1.22	41.11			28.75	28.75	1.99
ap	0.71	0.16		1.6	0.89	0.46	6.72	2.29	3.54		0.16	0.91	3.26	0.16		0.74		1.20	1.58
anh								32.38	42.83										
il	0.87	0.21	0.64	2.13	1.56	1.83	1.38	0.76	2.08		0.65	0.11	1.33	0.98		0.91	0.41	0.02	0.23
mt	0.49	0.05	0.21	0.89	0.06	0.4	0.52	0.57	0.9	0.05	0.16	0.28	0.5	0.22	1.80	1.02	0.36	0.02	0.23
ol	18.63	45.85	23.57	41.05	20.74	21.61	21.7				0.49	47.59	21.49		96.60	27.5			24.23
cpx		16.71	9.62	36.97		50.31	36.74	34.19	33.21	28.06	67.78		12.82	46.24		66.16	45.61	64.58	59.77
pl	3.38					11.61	11.37					1.87	6.91						
alkfels	46.57	33.26	8.55	16.29	71.07	11.15	3.44	9.29	6.84	3.4	6.76	40.79	52.49	0.55	1.60	3.68	2.29	6.74	11.99
ne	17.81											7.99							
qz								1.19	8.25	19.49				10.74			22.6	4.1	

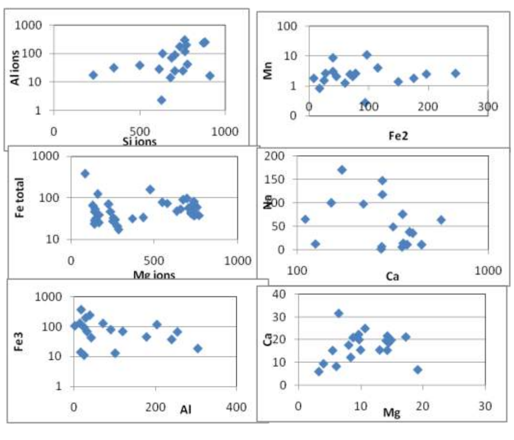

Fig:- 4. Plots of ions present in ultramafic (Table1)

Table:2a EDAX spot analyses ultramafic samples from arc shaped exposure :

	1	2	3	4	5	6	7	8	9	10	11	12	13	14	15	16	17	18	19	20
SiO2	37.86	9.22	42.08	44.95	42.53	42.47	44.52	44.94	30.05	40.22	39.77	38.81	32.16	47.52	45.81	46.33	46.76	46.41	16.04	34.34
Al2O3	37.76	14.22	34.42	35.65	35.38	35.47	31.80	31.95	28.81	31.58	33.40	33.10	47.45	37.93	39.10	33.42	32.85	34.71	59.12	47.25
Fe2O3																				
FeO	5.02	27.48	4.63	2.27	2.83	3.34	2.18	2.15	8.80	3.37	4.71	3.85	2.38	1.71	1.81	1.25	1.49	2.05	2.43	2.01
Mno																				
MgO	9.05	3.33	5.31	5.97	6.77	5.60	10.60	10.58	6.35	9.55	5.15	5.79	10.30	5.73	6.71	11.41	11.17	5.62	17.44	10.17
CaO	0.36	0.00	1.49	0.60	0.92	1.00	0.39	0.63	1.52	0.81	1.25	1.36	0.52	0.71	0.54	0.38	0.48	0.95	0.31	0.29
Na2O	0.15	0.00	0.18	0.26	0.31	0.08	0.09	0.17	0.23	0.00	0.00	0.00	0.50	0.00	0.00	0.00	0.00	0.31	0.32	0.14
K2O	0.40	0.14	1.40	0.91	1.12	1.08	0.35	0.56	1.36	0.83	1.30	1.43	0.68	1.02	0.66	0.46	0.43	0.72	0.28	0.44
TiO2	0.24	0.34	0.61	0.00	0.34	0.54	0.17	0.55	1.01	0.64	0.58	0.24	0.33	0.21	0.18	0.24	0.32	0.31	0.37	0.03
Sc2O3	0.05	0.20	0.82	0.37	0.47	0.64	0.41	0.52	1.42	0.71	0.58	0.69	0.48	0.35	0.38	0.34	0.47	0.47	0.28	0.13
Cr2O3	0.21	0.88	0.76	0.26	0.32	0.56	0.34	0.39	1.20	0.56	0.62	0.70	0.33	0.29	0.17	0.33	0.30	0.45	0.27	0.27
CoO	0.17	2.10	0.78	0.28	0.40	0.54	0.36	0.44	0.86	0.63	0.57	0.60	0.31	0.32	0.23	0.39	0.27	0.31	0.17	0.18
NiO	0.00	2.01	0.36	0.37	0.42	0.34	0.41	0.37	0.55	0.54	0.44	0.61	0.12	0.13	0.22	0.25	0.26	0.53	0.22	0.20
CuO	0.00	0.68	0.41	0.21	0.14	0.22	0.25	0.23	0.47	0.40	0.39	0.31	0.12	0.10	0.25	0.19	0.23	0.37	0.07	0.05
Rb2O	1.93	9.14	1.18	1.05	1.52	1.40	0.91	0.75	3.32	1.92	1.11	1.85	0.66	0.23	0.40	0.61	0.79	0.77	0.34	0.49
SrO	2.48	12.15	1.42	1.73	2.18	2.59	1.70	1.41	4.27	2.70	3.80	3.44	0.68	0.87	0.90	0.29	0.65	1.32	0.00	0.70
Y2O3	2.42	18.09	2.22	2.75	2.74	2.65	1.87	1.31	6.78	2.70	4.45	4.29	0.34	0.42	1.15	0.44	0.54	0.00	0.00	0.62
P2O5	0.00	0.00	0.00	0.00	0.22	0.24	0.00	0.11	0.29	0.00	0.00	0.33	0.20	0.40	0.39	0.53	0.40	0.53	0.00	0.52
SO3	0.08	0.00	0.17	0.00	0.16	0.49	0.10	0.34	0.49	0.43	0.11	0.45	0.54	0.34	0.32	0.58	0.46	0.65	0.37	0.44
F	0.26	0.00	0.40	0.60	0.12	0.43	0.21	0.31	0.66	0.61	0.42	0.32	0.83	0.58	0.49	0.21	0.26	0.52	0.78	0.75
Cl	0.03	0.00	0.32	0.11	0.14	0.32	0.10	0.23	0.33	0.20	0.11	0.28	0.28	0.31	0.27	0.26	0.24	0.33	0.15	0.11
CO2	1.54	0.00	1.02	1.66	0.98	0.00	3.26	2.09	1.21	1.60	1.22	1.54	0.77	0.83	0.00	2.07	1.64	2.67	1.02	0.87

	1	2	3	4	5	6	7	8	9	10	11	12	13	14	15	16	17	18	19	20
Ba	740	540	1150	1070	800	850	970	550	3230	1260	1180	1480	410	550	470	690	310	850	70	540
La	280	450	1420	730	780	1000	870	1100	2020	980	940	1270	750	570	510	540	900	430	510	340
Ce	300	940	1260	320	540	1070	800	760	2120	1130	1060	800	550	610	530	440	830	320	480	260
Nd	160	1220	680	480	330	590	430	630	1050	910	610	780	450	480	430	610	490	360	270	410
Eu	360	1120	930	540	700	1120	760	1060	2320	1010	1120	1050	620	630	400	670	820	780	310	150
Dy	1080	6110	1290	900	580	1370	1280	810	2060	1400	1320	790	450	700	770	690	610	1140	910	820
Yb	330	0	970	200	250	780	270	270	610	150	1000	0	640	470	460	390	800	380	340	330
Lu	0	1170	820	590	600	810	850	560	350	570	550	790	490	690	620	590	660	480	540	460
Hf	220	3070	810	640	580	980	880	680	770	560	280	730	490	300	620	530	470	630	550	370
Ta	470	1720	870	610	550	790	1000	910	1550	690	820	650	520	500	470	530	710	560	300	300
Au	790	4730	1640	1070	970	1970	1580	980	2730	2020	2360	2300	970	910	520	1010	1010	1000	580	750
Pb	0	4180	1640	1270	1820	1840	950	1070	1430	1310	1810	1550	650	1050	800	1130	1120	1050	0	1200
U	5080	13360	2900	2650	4270	4800	2510	2400	7990	3830	5910	4890	990	2560	2150	1110	550	1680	450	1610

Table:2b EDAX analyses ultramafic samples from arc shaped exposure

	1	2	3	4	5	6	7	8	9	10	11	12	13	14	15	16	17	18	19	20
cc	3.84		2.59	3.13	2.56		8.07	3	3.38	4.01	3.19	4	1.78	2.07			4.02	6.69	2.17	2.1
nakf	1.54		2.37	3.02	0.7		1.09	1.78			2.5									
nakcl			0.68		0.46						0.34									
mgf2				0.45					3.2			1.48	3.35	2.56	2.13	5.05	1.14	2.3	2.93	3.1
mgcl2	0.11			0.22		2.66	0.33	0.67	8.87			0.68	0.63	0.71	0.66	0.86	0.6	0.77	0.28	0.21
ap	0.44		0.5		0.46	0.45		0.28	0.66			0.74	0.42	0.87	0.88	1.13	0.87	1.04		1
anh	0.11		0.23		0.23		0.11	0.44	0.72	0.56		0.68	0.73	0.44	0.44	0.75		0.88	0.47	0.74
il	0.33	0.5	0.9		0.46	0.79	0.22	0.78	1.57	0.89	0.91	0.34	0.42	0.33	0.22	0.32	0.43	0.44	0.47	
mt	0.33	2.82	0.39	0.22	0.23	0.28	0.16	0.11	0.72	0.22	0.34	0.34	0.16	0.11	0.16	0.11	0.11	0.16	0.14	0.11
fesccry2	2.03	15.91	3.67	2.74	3.14	3.39	2.29	2.11	8.87	3.51	4.5	4.97	1.2	1.04	1.26	1.13	1.3	1.1	0.57	0.95
feconicu	0.16	8.02	2.26	1.34	1.51	1.81	1.42	1.56	2.9	2.23	2.16	2.28	0.84	0.76	0.99	1.08	1.09	1.76	0.57	0.63
ol	7.24	37.03							14				39.4						88.14	24.91
cpx	78.13		69.32	72.59	65.74	71	72.84	76.43	38.38	62.95	63.97	57.25	36.94	65.85	23.78	71.56	71.73	58.37		59.43
pl																			1.42	1.84
alkfels	5.76		7.61	3.07	17.71	14.13	2.73	2.22		18.11	15.37	23.69	14.13	12.27	9.85	7.26	8.68	9.87		4.99
ne		35.71							12.85										2.84	
qz			9.98	13.23	6.79	5.48	10.75	10.62		4.35	6.6	3.54		12.98	9.63	10.16	10.04	16.62		

	21	22	23	24	25	26	27	28	29	30	31	32	33	34	35	36	37	38	39	40
SiO2	22.57	55.71	58.66	61.22	56.80	53.33	56.69	53.34	56.10	56.12	59.15	61.20	61.86	60.44	59.85	58.34	59.87	57.41	58.17	58.17
Al2O3	53.93	4.07	1.26	1.43	1.75	5.42	2.00	2.86	2.96	1.37	0.65	2.21	1.14	0.95	0.93	3.39	1.84	2.65	3.18	3.18
Fe2O3																				
FeO	2.30	4.06	2.73	5.37	2.77	4.01	3.40	11.30	2.99	6.43	2.69	5.60	3.45	3.87	3.20	6.91	4.23	5.80	4.95	4.95
Mno																				
MgO	14.78	28.51	30.93	23.25	30.09	29.00	29.31	19.15	29.15	27.18	29.67	21.99	25.54	26.52	28.88	27.97	30.45	29.72	29.55	29.55
CaO	0.34	0.40	0.24	0.36	0.23	0.32	0.29	0.54	0.30	0.45	0.38	0.42	0.44	0.23	0.35	0.39	0.30	0.34	0.20	0.20
Na2O	0.20	0.54	0.56	0.55	0.68	0.39	0.48	0.71	0.90	0.66	0.64	0.74	0.65	0.17	0.58	0.40	0.37	0.38	0.76	0.76
K2O	0.33	0.30	0.26	0.48	0.18	0.32	0.37	0.71	0.38	0.30	0.35	0.48	0.42	0.18	0.28	0.22	0.21	0.23	0.07	0.07
TiO2	0.30	0.29	0.30	0.58	0.18	0.21	0.21	0.18	0.38	0.52	0.43	0.31	0.52	0.43	0.10	0.48	0.31	0.41	0.27	0.27
Sc2O3	0.34	0.36	0.38	0.63	0.26	0.35	0.32	0.86	0.31	0.39	0.36	0.49	0.69	0.33	0.57	0	0	0	0	0
Cr2O3	0.31	0.66	0.33	0.69	0.30	0.89	0.52	2.05	0.46	0.54	0.25	0.82	0.55	0.60	0.31	0	0	0	0	0
CoO	0.36	0.35	0.20	0.69	0.25	0.22	0.29	1.14	0.14	0.76	0.21	0.77	0.47	0.46	0.31	0	0	0	0	0
NiO	0.23	0.36	0.41	0.85	0.47	0.40	0.53	0.95	0.40	0.89	0.54	0.53	0.58	0.47	0.26	0	0	0	0	0
CuO	0.11	0.32	0.11	0.41	0.11	0.14	0.18	0.00	0.18	0.00	0.08	0.18	0.12	0.00	0.21	0	0	0	0	0
Rb2O	0.46	0.51	0.84	0.72	0.58	0.18	0.43	0.64	0.35	0.00	0.00	0.00	0.00	0.00	0.00	0	0	0	0	0
SrO	0.77	0.62	0.70	0.66	0.74	0.53	0.52	1.29	0.69	0.00	0.00	0.00	0.00	0.00	0.00	0	0	0	0	0
Y2O3	0.63	1.19	0.63	0.00	1.12	0.75	0.83	1.28	0.96	0.00	0.00	0.00	0.00	0.00	0.00	0	0	0	0	0
P2O5	0.18	0.28	0.00	0.51	0.32	0.21	0.17	0.24	0.54	0.00	0.64	0.93	0.53	0.56	0.00	0	0	0	0	0
SO3	0.45	0.36	0.54	0.62	0.40	0.54	0.41	0.60	0.72	0.00	0.62	0.71	0.44	0.82	0.38	0	0	0	0	0
F	0.28	0.87	0.70	0.62	1.08	1.36	0.89	0.65	0.99	1.25	1.56	0.13	0.83	1.63	1.30	0	0	0	0	0
Cl	0.24	0.22	0.23	0.34	0.12	0.24	0.21	0.36	0.29	0.18	0.30	0.68	0.35	0.17	0.40	0	0	0	0	0
CO2	0.88	0.00	0.00	0.00	1.59	1.18	1.96	1.14	0.81	2.96	1.47	1.80	1.42	2.18	2.10	1.90	2.42	3.07	0.14	0.14

	21	22	23	24	25	26	27	28	29	30	31	32	33	34	35
Ba	150	340	160	0	0	200	310	1500	0	490	0	940	90	0	600
La	520	870	480	1120	350	730	510	1500	570	1260	640	1670	560	930	530
Ce	680	350	400	1110	420	500	520	900	420	1250	420	940	820	800	600
Nd	280	590	270	620	350	520	380	1540	280	280	320	1050	730	450	400
Eu	520	530	450	980	260	620	570	990	670	1340	580	1970	860	700	580
Dy	760	1020	650	2030	1100	780	770	3880	680	1740	790	2650	1880	1570	770
Yb	200	210	190	630	0	200	0	900	0	1210	0	1230	0	870	750
Lu	540	390	360	670	240	360	720	1100	500	1220	520	1040	890	710	570
Hf	610	150	310	790	360	240	460	1810	390	810	150	760	350	780	350
Ta	610	420	430	1360	300	410	650	2260	410	1490	350	800	1070	640	450
Au	780	550	830	1540	930	780	660	2580	1090	1270	750	1310	1000	1140	780
Pb	720	650	960	1430	530	860	740	1600	800	1270	0	0	590	500	0
U	1420	1080	950	1700	610	1570	580	1180	650	0	780	1330	0	0	0

	21	22	23	24	25	26	27	28	29	30	31	32	33	34	35	36	37	38	*39*
cc	2.06				3.7	2.75	4.62	2.86	1.86	6.9	3.35	3.35	5.15	5.15	4.89	4.52	5.71	7.28	6.73
nakf											0.84				0.71				
nakcl																			
mgf2	1.18	3.60	2.9	2.64	4.37	5.39	3.65	2.81	4.03	5.1	2.73		6.64	6.64	4.74				
mgcl2	0.51	0.47	0.47	0.81	0.26	0.56	0.46	0.83	0.62	0.41	0.79		0.41	0.41	0.82				
ap	0.41	0.57		1.02	0.62	0.41	0.26	0.44	1.08		1.1	1.10	1.08	1.08					
anh	0.62	0.42	0.73	0.86	0.51	0.71	0.51	0.88	0.93		0.52	0.52	1.03	1.03	0.51				
il	0.41	0.42	0.41	0.75	0.21	0.31	0.31	0.22	0.52	0.72	0.63	0.63	0.51	0.51	0.10	0.63	0.42	0.52	*0.31*
mt	0.05	0.31	0.21	0.43	0.21	0.31	0.26	1.05	0.21	0.52	0.26	0.26	0.26	0.26	0.25	0.53	0.31	0.42	*0.36*
fesccry2	1.18	2.03	1.24	1.56	1.39	1.88	1.49	4.41	1.5	1.08	0.66	1.42	1.08	1.08	0.92				
feconicu	0.93	1.46	0.93	2.69	1.03	0.71	1.34	3.08	0.93	2.27	1.12	1.68	1.24	1.24	1.02				
ol	84.61																		
cpx	3.14	75.80	78.01	58.94	71.26	71.05	70.04	58.87	71.4	64.19	67.07	60.90	59.32	59.32	66.94	81.49	79.85	79.82	*78.46*
pl		1.56																	
alkfels	4.89	2.56	7	11.31	8.74	5.6	7.19	12.39	10.58	6.96	3.3	5.77	2.57	2.57	4.58	4.73	4.15	4.42	*6.99*
ne																			
qz		5.79	8.09	18.97	7.71	4.33	9.87	12.17	6.35	11.85	14.41	20.02	20.7	20.7	14.52	8.1	9.55	7.54	*7.15*

Saturated norm enriched with sillimanite might have been yield biotite in wet condition or garnet in dry state depending up on its environmental condition. Al’” against Si; Ca vs Mg and K vs Na show negative correlation while (Fe+Co+Ni+Cu) vs (Fe’”+Cr+Sc+Y) show positive variation. Fig- 5 shows that most of trace elements trend positively along narrow linear direction.

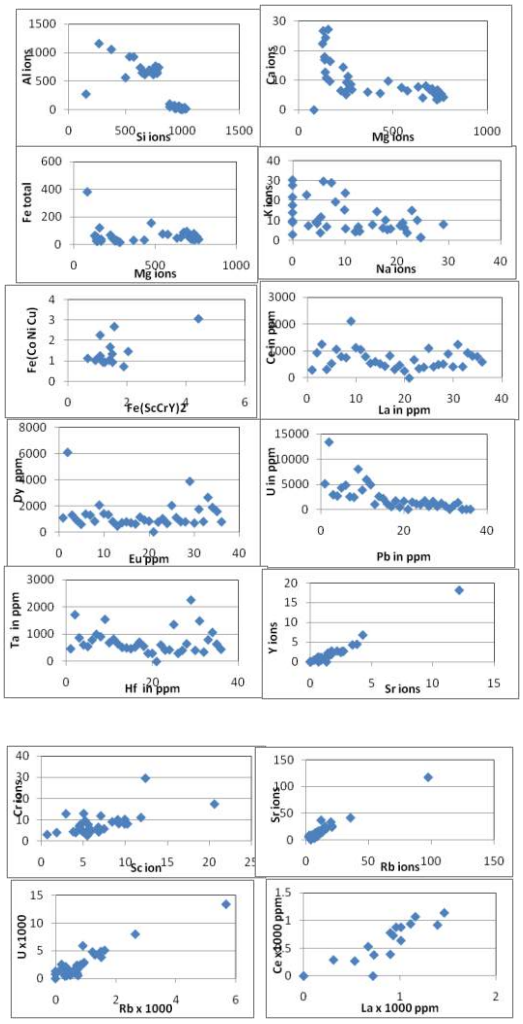

Fig. 5 Plots of EDAX spot analyses (Table-2a &2b)

5. DISCUSSION

Tschermak's molecule is an important end member in pyroxene group in which Al dominates in M1 and T sites. Al content of pyroxene increases with ensuing silica deficiency, increasing temperature and pressure. Sillimanite content in saturated norm in ***um***, is increased volume content of biotite, spinel, cordierite, corundum and garnet at high PT conditions [10]. Plagioclase is found in peridotite / pyrolite as accessory mineral [11] and has a solid solution between anorthite and albite. At high PT, plagioclase transforms into tschermakite releasing quartz. Highly aluminous ***um*** develops by break down of anorthite. Pyroxene breaks down into two series of subsolidus differentiation composing two end members of diopside-jadeite and diopside-acmite series in ***um*** [12]. Thus, ***um*** might have been produced both alkaline series and calc- alkaline series of rocks by subsolidus differentiation from low velocity zone of the Earth. The rocks in low velocity zone can be relatively less rigid than upper or lower zones.

Formation of riebeckite in syenite indicates that it is formed under high pressure state. Primary calcite reacts with tschermakite producing alumina rich melilite (gehlenite) which is characteristic mineral component in silica under saturated ultrabasic belonging to carbonatite complex. Melilite bearing xenoliths were reported in some of carbonatite complexes from South Africa [13]. Again, reactions of OH, CO_2, F, Cl, P_2O_5 and SO_3 from volatile phase produce primary melilite / scapolite group of minerals. Gehlinite / meionite are present in alkali syenite exposed adjacent to carbonatite and ***um***. Decompositions of phlogopite into vermiculite is seen in some parts of ***um.*** Nioborutile and hercynite reveal for Al"' enrichment in these rocks. Al"' enrichment in ***um*** takes place in the following reactions under high PTX conditions:

Anorthite – Quartz = Tschermakite
Albite –Quartz = Jadeite
Albite + Nepheline = 2 Jadeite
4 Anorthite + 6 Hypersthene – 2 Quartz = Tschermakite (amphibole)
4 Acmite + 6 Hypersthene + 2 Quartz = 2 Riebeckite
Low pressure minerals in crust = High pressure minerals in mantle

In appropriate PTX, , the minerals in the left hand side are may be replaced into high pressure mantle state. Reversible transition may be attributed with certain irregularities in some changes of cruatal rocks and minerals transforming into peridotite (***um).***

The peridotite / pyroxenite (***um***) from mantle region can be produced all types series of melilite, carbonatite, scapolite, alkaline and granitic rocks. Mantle at low velocity zone is highly heterogeneous. It may be composed of 0.05 to 0.1 per cent volatile content [14]. These rocks are subjected both confined and volatile pressures and these pressures locally vary place to place in three dimensional proportion. Subsolidus phase replacement cationic movement takes rapidly under variation in PTX. Transition of end member of tschermakite molecules from pyroxene into tschermakite amphibole releases quartz at high pressure. Many cases quartz is either released or consumed in the above transitions. The common characteristic minerals found in ***um*** are biotite, hornblende (tschermakite), spinel, nioborutile, REE minerals calcite, apatite, riebeckite, and apatite. Al"' enrichment in ***um*** at mantle region plays critical role for PTX under subsolidus differentiation of mantle to crust.

6. CONCLUSION

It appears that most of rocks and minerals that are found on the Earth's crust are derived from mantle source. Tectonic uplift, magmatic emplacement ultramafic xenoliths incorporated in magma or during upward movements from mantle to crust may be caused changes in PTX leading to subsolidus high or low pressure phase transformation. The low PTX might have been one of the causes for crustal evolution from mantle source. Alumina or alkali concentration in ***um*** in mantle leads to two different trends of subsolidus differentiates at different PTX condition as calc-alkaline and alkaline series. Volatile pressure locally affects as inclusion / bubble in low velocity zone is also played critical role in mineral phase differentiation at mantle. No adequate experiment or field evidence is available to prove that crust is a differentiated product from subsolidus mantle materials.

AKNOWLEDGEMENT

The author gratefully acknowledges Mr. V. Gopal, the Former State Geologist., who showed me the presence of native copper, silver, sulphide and carbonate minerals in the nodule. He thanks Dr, V. Subramayam, former Deputy Director, Tamil Nadu State Geology Branch, for identification monazite and REE minerals in myrolytic and aplitic pegmatite adjacent to the skarn rock body in the field. He thanks to Mr. T. Ragavaiyya, Senior Technician in the Laboratory of Material Sciences, IITM, Chennai-36 for his co-operation during the course of Laboratory investigation.

List Item – 1 Article with 8pages
List Item – 2.Fives figures
List Item – 3: 14 References
List Item – 4: Author's bibliography with photo

REFERENCES

[1] I. S. Borodin, V. Gopal, V. M. Maralev, V. Subramanian, Precambrian carbonatites of Tamil Nadu, South India, *Journal of the Geological Society of India,* v. 12, pp.101-112, 1973

[2] R. Ramasamy, Geology of the area South west of Tiruppattur, Madras State (Tamil Nadu), India, Ph.D., Thesis, pp226, University of Madras, 1973

[3] R. Ramasamy, Structure and tectonics of carbonatite complex of Tiruppattur, Tamil Nadu In: A.K. Bhattacharya, (Ed.) *Current Trends in Geology, IV Indian Geological Congress,* Today and Tomorrows Publishers, New Delhi, pp. 119-136, 1982

[4] R. Ramasamy, Crystallization, fractionation and solidification of co-magmatic alkaline series sequentially emplaced in carbonatite complex of Tiruppattur, Tamil Nadu, India, Book on Crystallization- Science and Technology, Edrs Marcello Rubens, Barsi Andreeta, ISBN, pp. 535-564, 12th Sept. 2012, *INTECH*, Austria.

[5] S. Saravanan, S. and Ramasamy A magnesio-riebeckite from Samalpatti area, Tamil Nadu, India, *Mineralogical Magazine, v. 38, pp. 376-377, 1971*

[6] S. Saravanan, and R. Ramasamy, Geochemistry and petrogenesis of shonkinite and associated alkaline rocks of Tiruppattur carbonatite complex, Tamil Nadu, *Journal of the Geological Society of India, v. 46, pp. 235-243, 1995.*

[7] R. Ramasamy, Icelandspar Ocelli from skarn rock of Garigaipalli area, Tamil Nadu, *Current Sci*.v.52, (17) Sept., pp.808-811, 1983

[8] R. Ramasamy, S.P. Subramanaian, and R. Sundaravadivelu, R. Compositional variations of olivine in shonkinite and its associate ultrabasic rock from the carbonatite complex of Tiruppattur, Tamil Nadu,

[9] R. R.amasamy, L.G. Gwalani, and S.P. Subramanian, A note on the occurrence and formation of magnetite in the carbonatites of Sevvattur, North Arcot district, Tamil Nadu, Southern India Journal of Asian Earth Sciences, v. 19, pp 297-304, 2001.

[10] A. Rittmann, Stable Mineral Assemblages of Igneous Rocks, Springer-Verlag, Berlin, 264p, 1973.

[11] Don L. Anderson, *New Theory of the Earth, Cambridge University Press, 2nd Edn, p. 193, 2007*

[12] M. Morimoto. Composition ranges and nomenclature of the common (Ca-Mg-Fe) and Na and Fe"' pyroxene, Min.Mag. v. 52 pp 535-550, 1988

[13] Verwoerd, W.J. South African Carbonatites and their probable mode of origin, Ph.D. Thesis, Univ. of Stellenboch, 1966

[14] Amir Khan, On Earth's Mantle Constitution and Structure from Joint Analysis of Geophysical and Laboratory-Based Data: An Example, Surv. Geophysics, DOE 100: 1007s10712-015-9353z 2016.

AUTHORS' BIOGRAPHIES

Ph.D. Univ. Madras 1974, PDF Geochim in MSU, Russia 77-80. Petrologist in DGM 74-2000, Project Consultant in DOE & CE IITM 2008-15,